

ISSN 1561-2430 (Print)  
ISSN 2524-2415 (Online)  
UDC 621.383:539.1.43

<https://doi.org/10.29235/1561-2430-2018-54-3-360-368>

Received 11.05.2018

Поступила в редакцию 11.05.2018

**I. A. Romanov<sup>1</sup>, I. N. Parkhomenko<sup>1</sup>, L. A. Vlasukova<sup>1</sup>, F. F. Komarov<sup>2</sup>,  
N. S. Kovalchuk<sup>3</sup>, O. V. Milchanin<sup>2</sup>, M. A. Makhavikou<sup>2</sup>, A. V. Mudryi<sup>4</sup>,  
V. D. Zhivulko<sup>4</sup>, Hong-Liang Lu<sup>5</sup>**

<sup>1</sup>Belarusian State University, Minsk, Belarus

<sup>2</sup>A. N. Sevchenko Institute of Applied Physical Problems of the Belarusian State University, Minsk, Belarus

<sup>3</sup>Joint Stock Company "Integral" Minsk, Belarus

<sup>4</sup>Scientific and Practical Materials Research Center of the National Academy of Sciences of Belarus,  
Minsk, Belarus

<sup>5</sup>State Key Laboratory of ASIC and System, School of Microelectronics, Fudan University, Shanghai, China

## BLUE AND RED LIGHT-EMITTING NON-STOICHIOMETRIC SILICON NITRIDE-BASED STRUCTURES

**Abstract.** The two triple-layered SiO<sub>2</sub>/SiN<sub>x</sub>/SiO<sub>2</sub> structures with Si-rich and N-rich silicon nitride active layer were fabricated on *p*-type Si-substrates by chemical vapour deposition. The SiN<sub>x</sub> layer of different composition ( $x = 0.9$  and  $x = 1.4$ ) was obtained by changing the ratio of the SiH<sub>2</sub>Cl<sub>2</sub>/NH<sub>3</sub> flow rates during deposition of a silicon nitride active layer (8/1 and 1/8, respectively). The spectroscopic ellipsometry and photoluminescence (PL) measurements showed that the refractive index, the absorbance and luminescence properties depend on a chemical composition of silicon nitride layers. The structures with Si-rich and N-rich SiN<sub>x</sub> active layers emit in the red (1.9 eV) and blue (2.6 eV) spectral ranges, respectively. The PL intensities of different structures are comparable. The rapid thermal annealing results in the intensity decrease and in the PL spectra narrowing in the case of SiN<sub>1.4</sub> active layer, whereas the increase in the emission intensity and the PL spectra broadening are observed in the case of the annealed sample with a SiN<sub>0.9</sub> active layer. The PL origin and the effect of annealing treatment have been discussed, taking into account the band tail mechanism of radiative recombination. Multilayered (SiO<sub>2</sub>/SiN<sub>x</sub>)<sub>n</sub>/Si structures are of practical interest for creation of effective light sources on the basis of current Si technology.

**Keywords:** non-stoichiometric silicon nitride, photoluminescence, spectral ellipsometry, absorption edge, rapid thermal annealing

**For citation.** Romanov I. A., Parkhomenko I. N., Vlasukova L. A., Komarov F. F., Kovalchuk N. S., Milchanin O. V., Makhavikou M. A., Mudryi A. V., Zhivulko V. D., Hong-Liang Lu. Blue and red light-emitting non-stoichiometric silicon nitride-based structures. *Vestsi Natsyianal'nai akademii navuk Belarusi. Seryia fizika-matematychnykh navuk = Proceedings of the National Academy of Sciences of Belarus. Physics and Mathematics series*, 2018, vol. 54, no. 2, pp. 360–368. <https://doi.org/10.29235/1561-2430-2018-54-3-360-368>

**И. А. Романов<sup>1</sup>, И. Н. Пархоменко<sup>1</sup>, Л. А. Власукова<sup>1</sup>, Ф. Ф. Комаров<sup>2</sup>, Н. С. Ковальчук<sup>3</sup>,  
О. В. Мильчанин<sup>2</sup>, М. А. Моховиков<sup>2</sup>, А. В. Мудрый<sup>4</sup>, В. Д. Живулько<sup>4</sup>, Хонг-Ланг Лу<sup>5</sup>**

<sup>1</sup>Белорусский государственный университет, Минск, Беларусь

<sup>2</sup>Институт прикладных физических проблем им. А. Н. Севченко Белорусского государственного университета,  
Минск, Беларусь

<sup>3</sup>ОАО «Интеграл», Минск, Беларусь

<sup>4</sup>Научно-практический центр Национальной академии наук Беларуси по материаловедению, Минск, Беларусь

<sup>5</sup>Школа микрорелектроники Фуданского университета, Шанхай, Китай

## СВЕТОИЗЛУЧАЮЩИЕ СТРУКТУРЫ НА ОСНОВЕ НЕСТЕХИОМЕТРИЧЕСКОГО НИТРИДА КРЕМНИЯ

**Аннотация.** Методом химического газофазного осаждения на кремниевых подложках *p*-типа изготовлены две трехслойные структуры SiO<sub>2</sub>/SiN<sub>x</sub>/SiO<sub>2</sub> с нестехиометрическими пленками нитрида кремния, обогащенными кремнием ( $x = 0,9$ ) или азотом ( $x = 1,4$ ), в качестве активных слоев. Активные слои SiN<sub>x</sub> нестехиометрического состава ( $x = 0,9$  и  $x = 1,4$ ) получены при различном соотношении реагирующих газов (SiH<sub>2</sub>Cl<sub>2</sub>/NH<sub>3</sub>) в процессе осаждения (8/1 и 1/8 соответственно). Методами спектральной эллипсометрии и фотолюминесценции показано, что показатель преломления, поглощение и люминесцентные свойства зависят от стехиометрического состава нитрида кремния. Структуры с активными слоями нитрида с избытком кремния и азота излучают в красной (1,9 эВ) и синей (2,6 эВ) областях спектра соответственно, причем интенсивность свечения сравнима для двух образцов. Быстрая термическая обработка приводит к уменьшению интенсивности и сужению спектра фотолюминесценции образца с активным

слоем  $\text{SiN}_{1.4}$ , тогда как для образца с активным слоем  $\text{SiN}_{0.9}$  наблюдается возрастание интенсивности люминесценции с уширением спектра в коротковолновую область после отжига. Природа видимого свечения и влияние термообработки объясняются с учетом существования протяженной зоны хвостовых состояний.

Структуры с чередующимися слоями оксида и нитрида кремния представляют практический интерес для создания эффективных источников света на базе кремниевой технологии.

**Ключевые слова:** нестехиометрический нитрид кремния, фотолюминесценция, спектральная эллипсометрия, край поглощения, быстрый термический отжиг

**Для цитирования.** Светоизлучающие структуры на основе нестехиометрического нитрида кремния / И. А. Романов [и др.] // Вест. Нац. акад. наук Беларусі. Сер. фіз.-мат. навук. – 2018. – Т. 54, № 3. – С. 360–368. <https://doi.org/10.29235/1561-2430-2018-54-3-360-368>

**Introduction.** At present, covering the full range of visible spectrum light-emitting diodes based on III-nitride semiconductors (GaN, InN, AlN, InGaN) have high efficiency, long lifetimes and commercially availability. But, there is still a problem of designing of light source compatible with the existing Si technology to develop the full optical link in integrated circuits instead of conventional metallic interconnections. A logical solution to the problem of Si-based light source absent is a development of LEDs based on silicon nitride ( $\text{SiN}_x$ ). Indeed, amorphous silicon nitride is one of the most important dielectrics in the current planar silicon technology. It is widely used in the integrated circuit production as gate dielectric films in transistors, passivation and charge storage layers in nonvolatile memory. Recently, the light-emitting properties of amorphous silicon nitride films have been attracting researcher's interest. However, the researcher's efforts are mainly concentrated on non-stoichiometric Si-rich  $\text{SiN}_{x<1.3}$  films. Such films are used as a matrix for the light-emitting Si nanocrystal formation during deposition or annealing [1–2]. Afterwards, it was demonstrated that the origin of emission from  $\text{SiN}_x$  films should not be unambiguously assigned to the emission of Si nanoclusters synthesized in the silicon nitride matrix. Silicon nitride exhibits intrinsic light-emitting properties via presence of deep defect levels and continues band tail states in band gap [3–5]. Besides, the optical properties of  $\text{SiN}_x$  films can be controlled by the variation of chemical composition. There are many previous studies that demonstrated the changing band gap, refractive index and absorption coefficient with variation of atomic ratio N/Si ( $x = 0\text{--}1.7$ ) of the non-stoichiometric  $\text{SiN}_x$  films [3, 6–15]. Mainly, these works were devoted to the hydrogen containing films deposited by plasma-enhanced or photo-chemical vapor deposition (CVD), radio-frequency glow discharge at temperatures  $< 500$  °C. The similar studies of the low-hydrogen silicon nitride films deposited by radio frequency magnetron sputtering or low pressure CVD (LPCVD) techniques as well as studies devoted to  $\text{SiN}_x$  photoluminescence (PL) have been discussed only for Si-rich films ( $x < 1.3$ ) [3, 7–11, 16–21]. In this work, we studied optical properties of the structures with Si-rich and N-rich light-emitting  $\text{SiN}_x$  layer deposited by LPCVD. It was demonstrated that the N-rich ( $\text{SiN}_{x>1.3}$ ) silicon nitride can also be as an effective active layer in multilayered  $\text{SiO}_2/\text{SiN}_x/\text{SiO}_2$  structures.

**Experimental.** Two triple-layered  $\text{SiO}_2/\text{SiN}_x/\text{SiO}_2$  structures were fabricated on the commercial Cz-Si-substrates (*p*-type) by CVD techniques (Fig. 1). Before the deposition, silicon substrates were cleaned in an oxidizing bath. Stoichiometric silicon dioxide was deposited by plasma-enhanced chemical vapour deposition (PECVD) as a buffer and capping layer using a gaseous mixture of silane  $\text{SiH}_4$  (250 sccm) and nitrous oxide ( $\text{N}_2\text{O}$ ) (1166 sccm) as precursors at 350 °C. The pressure in the chamber was kept constant at 52 Pa. Non-stoichiometric silicon nitride ( $\text{SiN}_x$ ) was deposited on the buffer  $\text{SiO}_2$  layer by LPCVD at 830 °C as an interlayer. The total flow rate of reagent gas ( $\text{SiH}_2\text{Cl}_2 + \text{NH}_3$ ) and pressure were maintained at 135 sccm and 40 Pa, respectively. By changing a ratio of reagent gases flow rates ( $R = \text{SiH}_2\text{Cl}_2/\text{NH}_3$ ) in the reactor chamber, two structures differed by stoichiometric composition of active layer ( $x = [\text{N}]/[\text{Si}]$ , where  $[\text{N}]$  and  $[\text{Si}]$  are the nitrogen and silicon atomic concentrations) were deposited. The partial flow ratio ( $R$ ) of reagent gases was chosen as 8/1 and 1/8.

The atomic ratio ( $x$ ) of as-deposited  $\text{SiN}_x$  films was determined by Rutherford backscattering spectrometry using 1.5 MeV  $\text{He}^+$  ions from the HVE AN-2500 accelerator. The compositions of active  $\text{SiN}_x$  layer were  $\text{SiN}_{0.9}$  (Si-rich) and  $\text{SiN}_{1.4}$  (N-rich) for the films deposited at chosen  $R$  (8/1 and 1/8, respectively). Hereafter, the samples  $\text{SiO}_2/\text{SiN}_{0.9}/\text{SiO}_2$  and  $\text{SiO}_2/\text{SiN}_{1.4}/\text{SiO}_2$  are labeled as SRN and NRN ones. The  $1 \times 1$  cm<sup>2</sup> samples were cut out from the structures and undergone rapid thermal annealing (RTA) at 1200 °C for 3 min using the setup 'JetFirst-100'. The thicknesses of layers in the fabricated structures

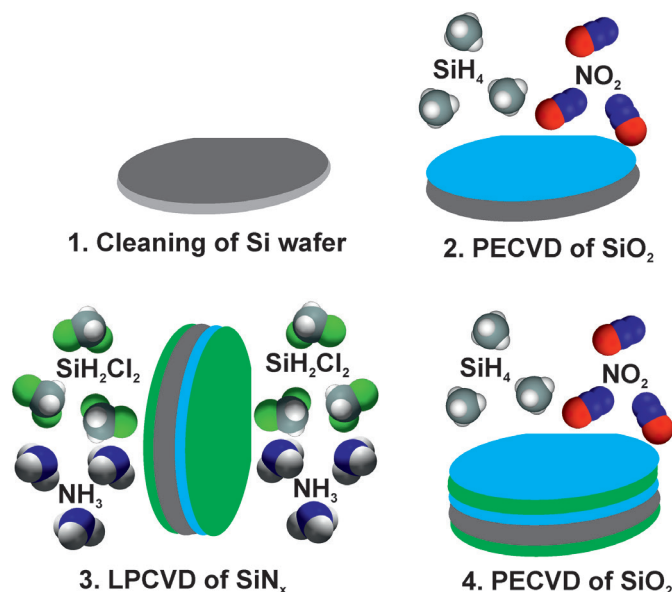


Fig. 1. Steps of CVD deposition of triple-layered SiO<sub>2</sub>/SiN<sub>x</sub>/SiO<sub>2</sub> on Si wafer

were investigated by scanning electron microscopy (SEM) using the Hitachi S-4800 microscope. Spectroscopic ellipsometry measurements of the refraction index ( $n$ ) and the extinction coefficient ( $k$ ) in the range of 200–1000 nm were performed using the spectroscopic ellipsometer HORIBA UVISEL 2. Photoluminescence (PL) spectra were recorded at room temperature in the spectral range of 350–800 nm with a He-Cd laser (325 nm) as excitation source using a home-made setup.

**Results and discussion.** Fig. 2 shows the SEM images of deposited films. Unfortunately, the interface between SiN<sub>x</sub> and SiO<sub>x</sub> layers were not revealed due to low contrast. As a result, SEM gave information only on a total thickness of the fabricated structures. The total thickness of triple-layered structure was equal to 126 nm and 212 nm for the SRN and NRN samples, respectively. However, the features of used deposition techniques (PECVD and LPCVD) could help to determine the depth of SiN<sub>x</sub> layer. Namely, during PECVD process the film is deposited only on one side of the wafer while during the LPCVD process film is deposited on both sides of wafer due to vertical design of the used furnace.

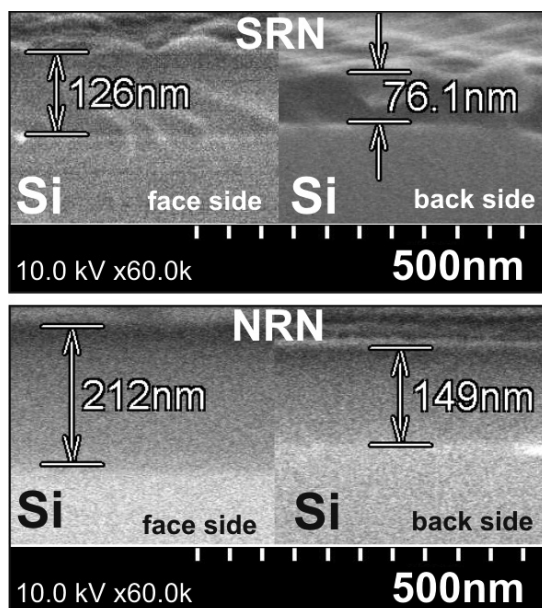


Fig. 2. SEM images of the SRN and NRN samples. The triple-layered SiO<sub>2</sub>/SiN<sub>x</sub>/SiO<sub>2</sub> structure was deposited on the face side of the Si substrate. Simultaneously, the SiN<sub>x</sub> layer of appropriate thickness was deposited on the back side of the Si substrate

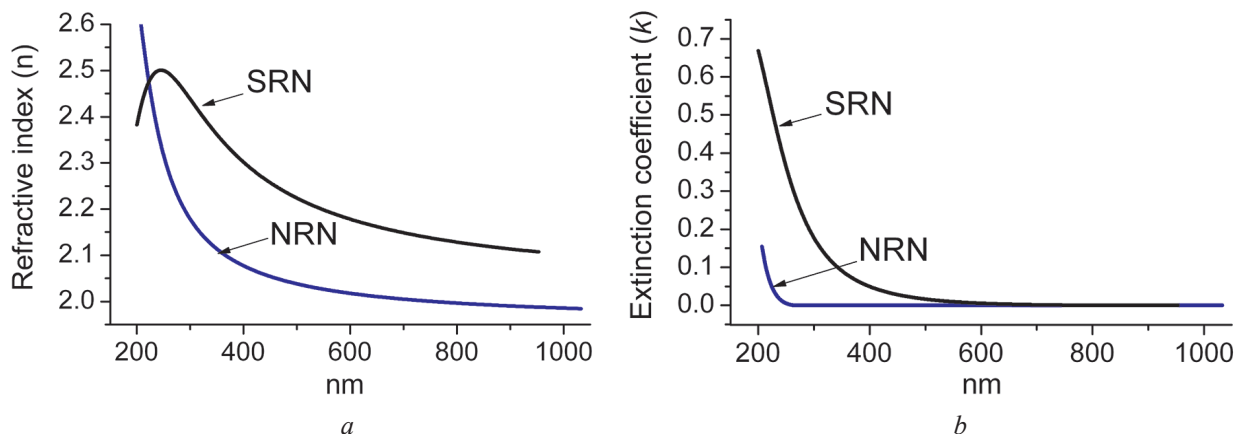


Fig. 3. Dispersion of the refractive index  $n(\lambda)$  (a) and the extinction coefficient  $k(\lambda)$  (b) of the as-deposited SRN and NRN structures

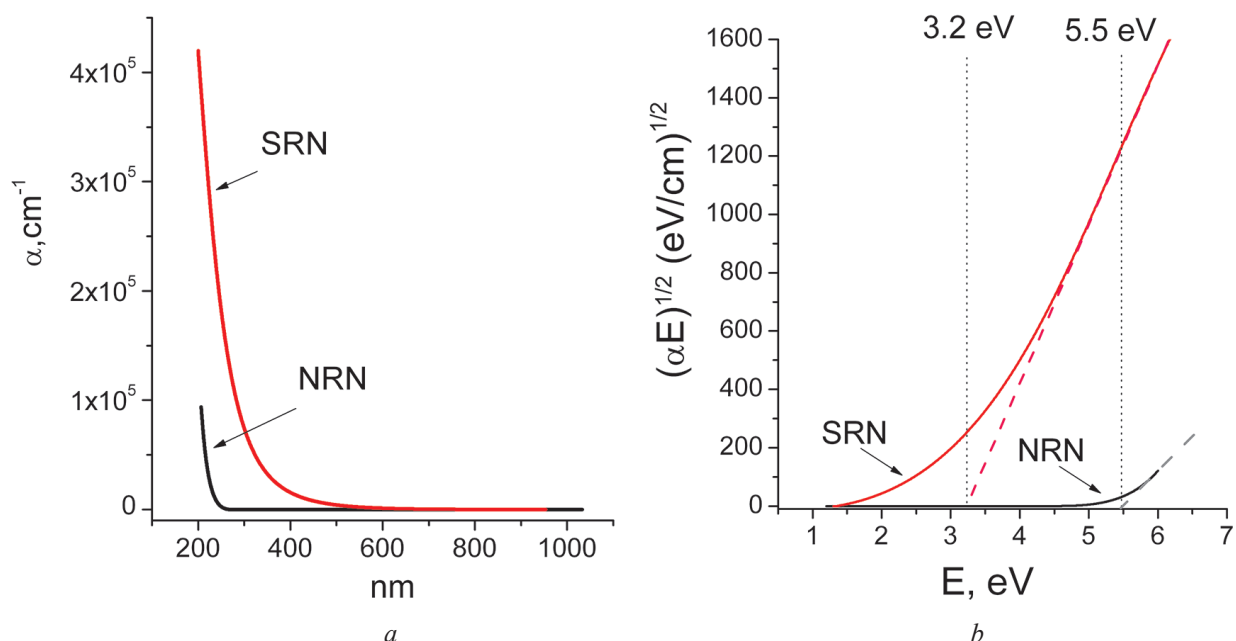


Fig. 4. Absorption coefficient spectra (a) and Tauc's plots of the SRN and NRN samples (b)

So, the single silicon nitride film of the same thickness as in the triple structure was deposited in the back side of Si wafer. Thus, the SEM images of wafer back side shows that the thickness of active  $\text{SiN}_x$  layer is equal to 76 nm and 149 nm for the SRN and NRN samples, respectively.

Fig. 3 shows the variation of optical constants such as the real part of the refraction index  $n(\lambda)$  and the extinction coefficient  $k(\lambda)$  of the SRN and NRN structures. As can be seen from Fig. 3, the optical properties of deposited structures depend on active layer composition. For the SRN structure, the refractive index has higher values in the visible spectral range. A similar trend of  $n$  increase with the increasing N/Si atomic ratio of  $\text{SiN}_x$  films has been shown in literature [13, 22–24]. It should be noted the anomalous behavior of  $n$  for the SRN structure in the range of (200–300 nm). It is typical for silicon nitride films with large excess of Si [22, 24]. The both obtained structures show the extinction coefficient amplitude increase to become nearby lower wavelengths (UV spectral range). The extinction coefficient  $k$  is quasi null for the wavelength higher than 610 nm and 250 nm for the SRN and NRN, respectively.

Fig. 4 shows the corresponding absorption coefficient  $\alpha$  calculated from the extinction coefficient ( $\alpha = 4\pi k/\lambda$ ).

It is evident the absorption edge blue shift with increasing  $x$  parameter. It indicates an optical band gap widening with increase of N/Si ratio. Assuming parabolic bands, the absorption edge could be determined using the well-known Tauc's equation:

$$(\alpha E)^{1/2} = B(E - E_g),$$

where  $E$ ,  $E_g$  and  $B$  are the photon energy, indirect optical gap and the Tauc constant (slope), respectively.  $E_g$  calculated by the straight line extrapolation in the linear region of Tauc's plots with the energy axis are equal to 3.2 eV and 5.5 eV for SRN and NRN structures, respectively. These values are differed with the  $E_g = 5$  eV of stoichiometric  $\text{Si}_3\text{N}_4$  deposited by LPCVD [25].

$E_g$  reduction with the decreasing N/Si ratio was reported for Si-rich films elsewhere [12, 15, 26] and explained via the progressive replacement of Si–N bonds by Si–Si bonds. The nonstoichiometric silicon nitride film is composed of a random network of Si–N and Si–Si bonds. In the case of Si-rich alloys, the band edges are formed by the Si–Si states. In the N-rich alloys, the replacement of Si–Si bonds by stronger Si–N bonds causes the band gap increase with the increasing stoichiometric parameter  $x$ .

Tauc slope  $B$  could provide information about the degree of spreading tails of valence and conduction bands [23]. The value of  $B$  determined from the Tauc's plots is equal to  $540 (\text{eV}\cdot\text{cm})^{-1/2}$  and  $245 (\text{eV}\cdot\text{cm})^{-1/2}$  for SRN and NRN structures, respectively. It is known that the width of band tail states can depend on static disorder due to structural randomness. In some papers [20, 27–28], band-tail states in the non-stoichiometric  $\text{SiN}_x$  films are attributed to a long-range disorder due to spatial fluctuations of the elemental composition. The dependence of  $B$  on stoichiometric parameter is not linear. In Ref [23], Si-rich and stoichiometric nitride films ( $x = 0.34\text{--}1.34$ ) were studied. According to [23] the minimal value of  $B$  is equal to  $130 (\text{eV}\cdot\text{cm})^{-1/2}$  for  $x = 1.34$ . The change of  $B$  for a wider range of  $x$  ( $x = 0\text{--}1.6$ ) was discussed in [26, 29]. In this case, a minimum in the Tauc slope ( $250 (\text{eV}\cdot\text{cm})^{-1/2}$ ) is at around  $x = 1.0$ . According to [14] the  $B$  decreases linearly with the increasing  $x$  from 0 to 1.5 and increases abruptly for the  $x > 1.5$ . The magnitude of  $B$  is inversely proportional to energy ranges occupied by tail states. In the case of investigated SRN and NRN structures, it can be concluded that both ones exhibit band tail states. However, NRN structure exhibits a more significant tailing.

Fig. 5 shows the room-temperature PL spectra of the as-deposited SRN and NRN samples. The position and full width at half maximum (FWHM) of the PL bands depend on the composition of active layer. The PL bands maxima are located in red range at  $\sim 1.9$  eV (650 nm) for the SRN sample and in blue range  $\sim 2.6$  eV (470 nm) for the NRN sample. PL bands are broader for the NRN films (FWHM is equal

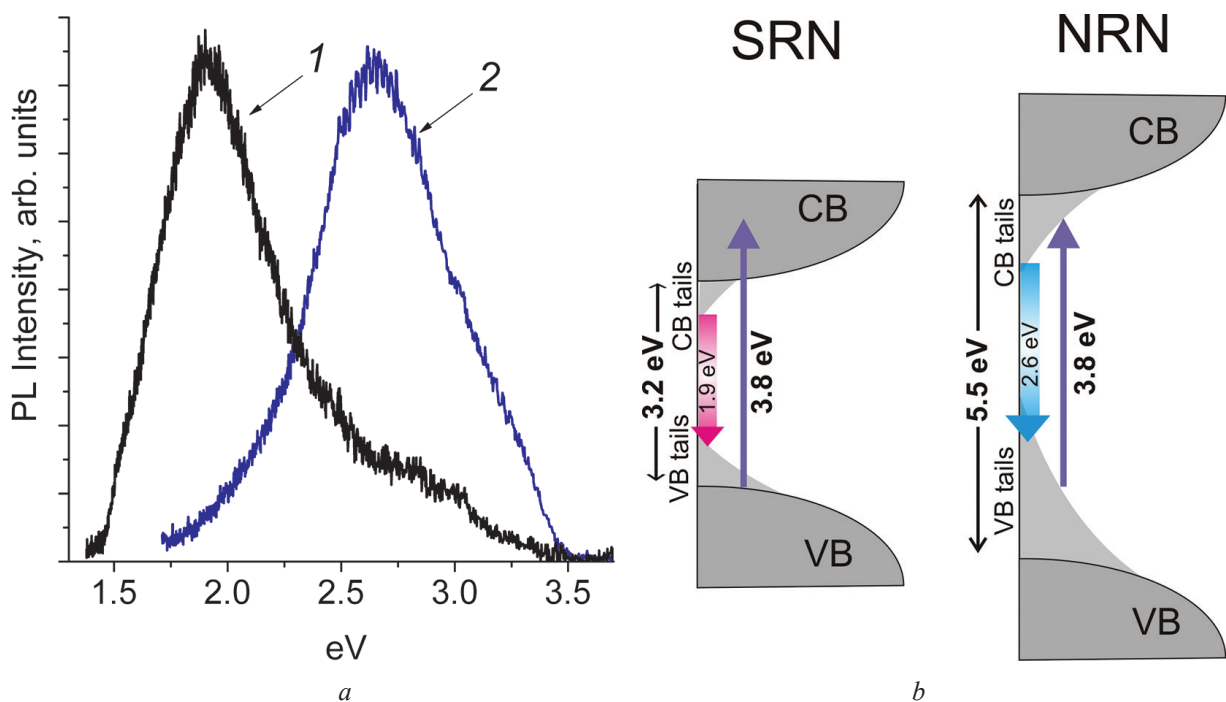


Fig. 5. PL spectra of the as-deposited SRN (1) and NRN (2) structures (intensity normalized to thickness) (a) and schematic energy band possible optical transitions for the both structures, assuming band tail states (b)



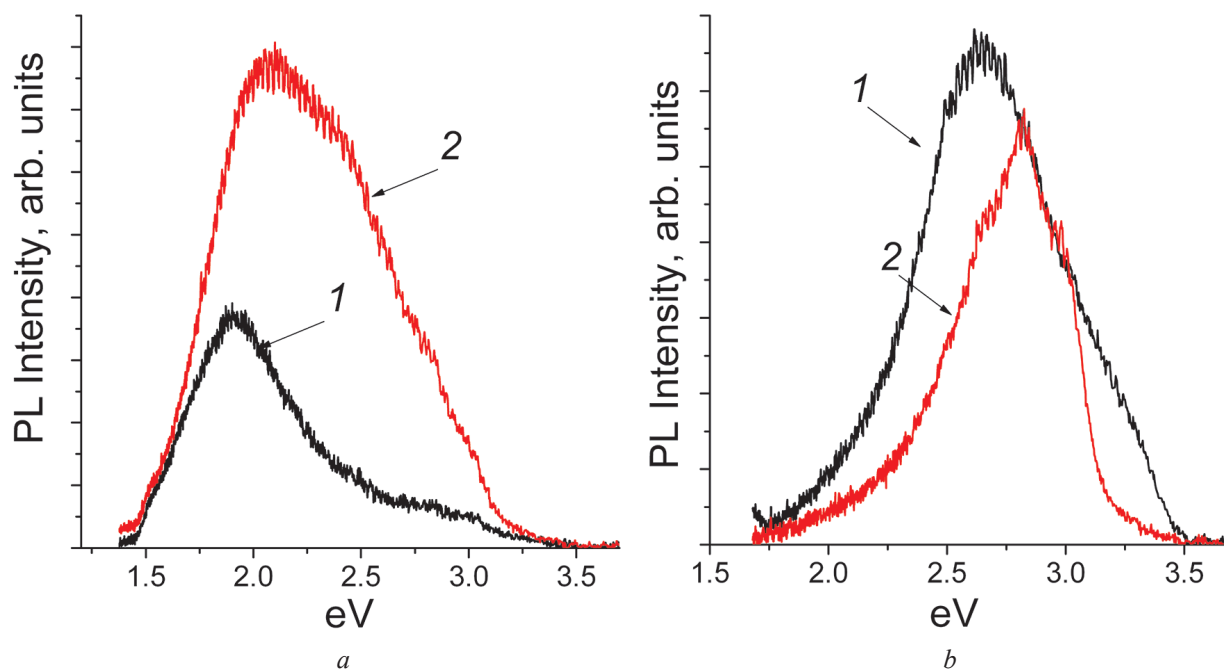


Fig. 6. PL spectra of the as-deposited (1) and annealed (2) SRN (a) and NRN (b) samples

to  $\sim 0.7$  eV) than for the SRN (FWHM is equal to  $\sim 0.6$  eV). It should be noted that an additional weak emission in blue spectral range is registered for the SRN structure.

Fig. 6 shows the effect of RTA on light-emitting properties of the structures. In the case of the structure with Si-rich silicon nitride as active layer (SRN sample), the annealing results in increase of PL intensity with the broadening to short wavelength range. On the contrary, the annealing of the structure with N-rich silicon nitride as active layer (NRN sample) leads to a negative effect on PL intensity. Besides, the PL spectra of NRN sample become narrower after annealing. It should be noted that blue shift of PL maximum after annealing is observed for both SRN and NRN samples.

The energy positions of the PL bands (1.9 and 2.8 eV) are quite far away from the band edges  $E_g$  calculated from the ellipsometry data (3.2 and 5.5 eV for SRN and NRN structures, respectively). This suggests that PL arises from radiative recombination via band tail and/or defect states. The blue shift of PL maximum as well as PL spectrum broadening with  $x$  increasing for  $\text{SiN}_x$  alloys are typical features of the emission via radiative recombination of within localized states at the band tail [20, 30]. Indeed, the shift of PL band to blue spectral range for the NRN sample in comparison with SRN one is caused by larger  $E_g$ . It was shown that the NRN structure possesses band tails broader than those observed for the SRN structure. It results in fact that PL spectra of NRN structures is broader in comparison with SRN ones.

Surprisingly, the intensity of PL spectra of the as-deposited SRN and NRN structures are comparable. Taking into account the band-tail origin of PL, there are two factors which influence negatively PL intensity of the samples. For NRN structures, the sub-gap excitation ( $E_{\text{exc}}$  (3.8 eV)  $<$   $E_g$  (5.5 eV)) is realized (Fig. 5, b). In this case, the absorption occurs only into the band tail-states, and weak absorption results in weak emission [3]. For SRN structures, the above-gap excitation ( $E_{\text{exc}}$  (3.8 eV)  $>$   $E_g$  (3.2 eV)) is realized (Fig. 5, b). In this case, all photons are absorbed, but photoexcited carriers thermalize toward the demarcation energy that result in increasing probability of non-radiative recombination [3]. It should be noted that an additional blue weak band in PL spectrum of SRN samples can be originated from the band-to band recombination without thermalization process involving band tail states. Thus, despite the same mechanism of luminescence for both structures the measured emission intensities are caused by different reasons. Besides, in the case of triple-layered structures  $\text{SiO}_2/\text{SiN}_x/\text{SiO}_2$ , the interference effects can also influence their emission intensities [31]. But, discussion of this effect is beyond the scope of our study.

The blue shifts of PL maxima observed for both structures after annealing can be explained by the widening band gap due to the band tail shrinking. In turn, elimination of band tail states is caused by “smoothing” out structural inhomogeneity after annealing. Indeed, band-tail states in the non-stoichiometric  $\text{SiN}_x$  films as well as in amorphous  $\text{SiO}_x$  films should be related to short-range disorder due to a spatial fluctuation of the elemental composition [32–33]. In the case of PECVD silicon nitride films characterized with high concentration of Si–H bonds, annealing at some regimes can cause an increase of Si dangling bonds via hydrogen effusion which results in increase of localized tail states. However, in the case of LPCVD silicon nitride films (the ones deposited at high temperature), additional annealing can result only in reduction of native defect and dangling bond density as well as degree of structural disorder. Therefore, decrease of band tail spread and band gap increase are expected after annealing in our experiment. It could explain a blue shift of PL maxima. Besides, in the case of SRN, it should increase the absorption of excited photons ( $E_{\text{exc}}$  approaches to  $E_g$ ) and, as a result, the PL intensity should increase, too. In the case of NRN structure, the opening band gap should result in reduction of absorption and constriction of band tail energy range involved in the recombination process. As a consequence, the emission and PL spectra should become weaker and narrower, respectively. It is in agreement with the annealing effect on luminescence observed for the SRN and NRN samples.

**Conclusions.** Two triple-layered structures  $\text{SiO}_2/\text{SiN}_{0.9}/\text{SiO}_2$  and  $\text{SiO}_2/\text{SiN}_{1.4}/\text{SiO}_2$  prepared by CVD method emit under the excitation by laser light (3.8 eV) in blue (2.8 eV) and red (1.9 eV) spectral ranges, respectively. The spectral ellipsometry investigation reveals the larger band edge of active nitride layer in the case of  $\text{SiO}_2/\text{SiN}_{1.4}/\text{SiO}_2$  (5.5 eV) in comparison with  $\text{SiO}_2/\text{SiN}_{0.9}/\text{SiO}_2$  (3.2 eV). Based on the calculated Tauc slope, it can be concluded that an energy range occupied by band tail states for the N-rich active nitride layer is larger in comparison with that for the Si-rich active layer. The correlation between features of energy-band structure and light-emitting properties suggests that the origin of luminescence can be mainly attributed to the band-tail recombination. Annealing has different effects on emission of the structures with Si-rich and N-rich active layers. The PL spectra become more intensive and wider for the  $\text{SiO}_2/\text{SiN}_{0.9}/\text{SiO}_2$  structure after annealing. On the other side, annealing results in the degradation of emission intensity and contraction of PL spectra of the  $\text{SiO}_2/\text{SiN}_{1.4}/\text{SiO}_2$  structure. This effect is also explained by the band tail mechanism of radiative recombination.

**Acknowledgments.** This research was partially sponsored by the Belarusian Republican Foundation for Fundamental Research (Grants No. F17KIG-007) and by the National Key R&D Program of China (No. 2016YFE0110700).

## References

- Rodríguez-Gómez A., Moreno-Rios M., García-García R., Pérez-Martínez A.L., Reyes-Gasga J. Role of the substrate on the growth of silicon quantum dots embedded in silicon nitride thin films. *Materials Chemistry and Physics*, 2018, vol. 208, pp. 61–67. <https://doi.org/10.1016/j.matchemphys.2018.01.032>
- Shuleiko D. V., Zaboltnov S. V., Zhigunov D. M., Zelenina A. A., Kamenskih I. A., Kashkarov P. K., Photoluminescence of Amorphous and Crystalline Silicon Nanoclusters in Silicon Nitride and Oxide Superlattices. *Semiconductors*, 2017, vol. 51, no. 2, pp. 196–202. <https://doi.org/10.1134/S1063782617020208>
- Kistner J., Chen X., Wenig Y., Strunk H. P., Schubert M. B., Werner J. H. Photoluminescence from silicon nitride – no quantum effect. *Journal of Applied Physics*, 2011, vol. 110, no. 2, p. 023520 (5 p.). <https://doi.org/10.1063/1.3607975>
- Hiller D., Zelenina A., Gutsch S., Dyakov S. A., Lopez-Vidrier L., Estrade S., Peiro F., Garrido B., Valenta J., Korinek M., Trojanek F., Maly P., Schnabel M., Weiss C., Janz S., Zacharias M. Absence of quantum confinement effects in the photoluminescence of  $\text{Si}_3\text{N}_4$ -embedded Si nanocrystals. *Journal of Applied Physics*, 2014, vol. 115, no. 20, p. 204301 (9 p.). <https://doi.org/10.1063/1.4878699>
- Parkhomenko I., Vlasukova L., Komarov F., Milchanin O., Makhavikou M., Mudryi A., Zhivulko V., Žuk J., Kopyciński P., Murzalinov D. Origin of visible photoluminescence from Si-rich and N-rich silicon nitride films. *Thin Solid Films*, 2017, vol. 626, pp.70–75. <https://doi.org/10.1016/j.tsf.2017.02.027>
- Kanicki J., Warren W. L. Defects in amorphous hydrogenated silicon nitride films. *Journal of Non-Crystalline Solids*, 1993, vol. 164-166, pp. 1055–1060. [https://doi.org/10.1016/0022-3093\(93\)91180-B](https://doi.org/10.1016/0022-3093(93)91180-B)
- Singh S. P., Srivastava P. Recent progress in the understanding of Si-nanostructures formation in  $a\text{-SiN}_x\text{:H}$  thin film for Si-based optoelectronic devices. *Solid State Phenomena*, 2011, vol. 171, pp. 1–17. <https://doi.org/10.4028/www.scientific.net/SSP.171.1>
- Torchynska T. V., Casas Espinola J. L., Vergara Hernandez E., Khomenkova L., Delachat F., Slaoui A. Effect of the stoichiometry of Si-rich silicon nitride thin films on their photoluminescence and structural properties. *Thin Solid Films*, 2015, vol. 581, pp. 65–69. <https://doi.org/10.1016/j.tsf.2014.11.070>

9. Mercaldo L. V., Esposito E. M., Veneri P. D., Rezgui B., Sibai A., Bremond G. Photoluminescence properties of partially phase separated silicon nitride films. *Journal of Applied Physics*, 2011, vol. 109, no. 9, p. 093512 (5 p.). <https://doi.org/10.1063/1.3575172>
10. Wang M., Xie M., Ferraioli L., Yuan Z., Li D., Yang D., Pavese L. Light emission properties and mechanism of low-temperature prepared amorphous  $\text{SiN}_x$  films. I. Room-temperature band tail states photoluminescence. *Journal of Applied Physics*, 2008, vol. 104, no. 8, p. 083504 (4 p.). <https://doi.org/10.1063/1.2996292>
11. Xie M., Li D., Wang F., Yang D. Luminescence properties of silicon-rich silicon nitride films and light emitting devices. *ECS Transactions*, 2011, vol. 35, no. 18, pp. 3–19. <https://doi.org/10.1149/1.3647900>
12. Koutsourelis M., Michalas L., Gantis A., Papaioannou G. A study of deposition conditions on charging properties of PECVD silicon nitride films for MEMS capacitive switches. *Microelectronics Reliability*, 2014, vol. 54, no. 9–10, pp. 2159–2163. <https://doi.org/10.1016/j.microrel.2014.08.002>
13. Necas D., Perina V., Franta D., Ohlidal I., Zemek J. Optical characterization of non-stoichiometric silicon nitride films. *Physical Status Solidi C*, 2008, vol. 5, no. 5, pp. 1320–1323. <https://doi.org/10.1002/pssc.200777767>
14. Maeda K., Umezumi I. Atomic micro structure and electronic properties of  $a\text{-SiN}_x\text{:H}$  deposited by radio frequency glow discharge. *Journal of Applied Physics*, 1991, vol. 70, no. 5, pp. 2745–2754. <https://doi.org/10.1063/1.350352>
15. Banerji N., Serra J., Chiussi S., Leo A. B., Pe Árez-Amor M. Photo-induced deposition and characterization of variable bandgap  $a\text{-SiN}_x\text{:H}$  alloy films. *Applied Surface Science*, 2000, vol. 168, no. 1–4, pp. 52–56. [https://doi.org/10.1016/S0169-4332\(00\)00583-3](https://doi.org/10.1016/S0169-4332(00)00583-3)
16. Debieu O., Nalini R. P., Cardin J., Portier X., Perriere J., Gourbilleau F. Structural and optical characterization of pure Si-rich nitride thin films. *Nanoscale Research Letters*, 2013, vol. 8, no. 1, p. 31. <https://doi.org/10.1186/1556-276X-8-31>
17. Wang M., Li D., Yuan Z., Yang D., Qun D. Photoluminescence of Si-rich silicon nitride defect-related states and silicon nanoclusters. *Applied Physics Letters*, 2007, vol. 90, no. 13, p. 131903 (3 p.). <https://doi.org/10.1063/1.2717014>
18. Wang X., Liu Y., Chen D., Dong L., Chen C. Photoluminescence of Si-rich  $\text{SiN}_x$  films deposited by LPCVD under different conditions. *International Journal of Modern Physics B*, 2007, vol. 21, no. 26, pp. 4583–4592. <https://doi.org/10.1142/S0217979207037995>
19. Volodin V. A., Bugaev K. O., Gutakovskiy A. K., Fedina L. I., Neklyudova M. A., Latyshev A. V., Misiuk A. Evolution of silicon nanoclusters and hydrogen in  $\text{SiN}_x\text{:H}$  films: Influence of high hydrostatic pressure under annealing. *Thin Solid Films*, 2012, vol. 520, no. 19, pp. 6207–6214. <https://doi.org/10.1016/j.tsf.2012.05.019>
20. Jackson W. A., Searly T. M., Austin I. G., Gibson R. A. Photoluminescence excitation studies of  $a\text{-SiN}_x\text{:H}$  alloys. *Journal of Non-Crystalline Solids*, 1986, vol. 77–78, pp. 909–912. [https://doi.org/10.1016/0022-3093\(85\)90808-7](https://doi.org/10.1016/0022-3093(85)90808-7)
21. Mohammed S., Nimmo M. T., Malko A. V., Hinkle C. L. Chemical bonding and defect states of LPCVD grown silicon-rich  $\text{Si}_3\text{N}_4$  for quantum dot applications. *Journal of Vacuum Science & Technology A: Vacuum, Surfaces, and Films*, 2014, vol. 32, no. 2, p. 021507 (7 p.). <https://doi.org/10.1116/1.4861338>
22. Krüchel C. J., Fülöp A., Ye Z., Andrekson P. A., Torres-Company V. Optical bandgap engineering in nonlinear silicon nitride waveguides. *Optics Express*, 2017, vol. 25, no. 13, pp. 15370–15380. <https://doi.org/10.1364/OE.25.015370>
23. Charifi H., Slaoui A., Stoquert J. P., Chaib H., Hannour A. Opto-structural properties of silicon nitride thin films deposited by ECR-PECVD. *World Journal of Condensed Matter Physics*, 2016, vol. 6, no. 1, pp. 7–16. <https://doi.org/10.4236/wjcmp.2016.61002>
24. Smietana M., Bock W. J., Szmidt J. Evolution of optical properties with deposition time of silicon nitride and diamond-like carbon films deposited by radio-frequency plasma-enhanced chemical vapor deposition method. *Thin Solid Films*, 2011, vol. 519, no. 19, pp. 6339–6343. <https://doi.org/10.1016/j.tsf.2011.04.032>
25. Joshi B. C., Eranna G., Runthala D. P., Dixit B. B., Wadhawan O. P., Vyas P. D. LPCVD and PECVD silicon nitride for microelectronics technology. *Indian Journal of Engineering and Materials Sciences*, 2000, vol. 7, pp. 303–309. URL <http://hdl.handle.net/123456789/24418>
26. Robertson J. Defects and hydrogen in amorphous silicon nitride. *Philosophical Magazine B*, 1994, vol. 69, no. 2, pp. 307–326. <https://doi.org/10.1080/01418639408240111>
27. Goirgis F., Vinegoni C., Pavese L. Optical absorption and photoluminescence properties of  $a\text{-Si}_{1-x}\text{N}_x\text{:H}$  films deposited by plasma-enhanced CVD. *Physical Review B*, 2000, vol. 61, no. 7, pp. 4693–4698. <https://doi.org/10.1103/PhysRevB.61.4693>
28. Austin I. G., Jackson W. A., Searle T. M., Bhat P. K., Gibson R. A. Photoluminescence properties of  $a\text{-SiN}_x\text{:H}$  alloys. *Philosophical Magazine B*, 1985, vol. 52, no. 3, pp. 271–288. <https://doi.org/10.1080/13642818508240600>
29. Hasegawa S., Matuura M., Kurata Y. Amorphous  $\text{SiN}_x\text{:H}$  dielectrics with low density of defects, *Applied Physics Letters*, 1986, vol. 49, no. 19, pp. 1272–1274. <https://doi.org/10.1063/1.97383>
30. Kato H., Kashio N., Ohki Y., Seol K. S., Noma T. Band-tail photoluminescence in hydrogenated amorphous silicon oxynitride and silicon nitride films. *Journal of Applied Physics*, 2003, vol. 93, no. 1, pp. 239–244. <https://doi.org/10.1063/1.1529292>
31. Dyakov S. A., Zhigunov D. M., Hartel A., Zacharias M., Perova T. S., Timoshenko V. Yu. Enhancement of photoluminescence signal from ultrathin layers with silicon nanocrystals. *Applied Physics Letters*, 2012, vol. 100, no. 6, p. 061908 (4 p.). <https://doi.org/10.1063/1.3682537>
32. Gritsenko V. A. Atomic structure of the amorphous nonstoichiometric silicon oxides and nitrides. *Physics-Uspekhi*, 2008, vol. 51, no. 7, pp. 699–708. <https://doi.org/10.3367/UFNr.0178.200807c.0727>
33. Gritsenko V. A., Novikov Yu. N., Chin A. Short-range order and charge transport in  $\text{SiO}_x$ : experiment and numerical simulation. *Technical Physics Letters*, 2018, vol. 44, no. 6, pp. 541–544. <https://doi.org/10.1134/S1063785018060196>



### Information about the authors

**Ivan A. Romanov** – Postgraduate Student of the Department of Physical Electronics and Nanotechnology, Junior Researcher in the Materials and Device Structures at the Micro- and Nanoelectronics Laboratory, Belarusian State University (1, Kurchatov Str., 220108, Minsk, Republic of Belarus). E-mail: romivan@bsu.by

**Irina N. Parkhomenko** – Ph. D. (Physics and Mathematics), Senior Researcher in the Materials and Device Structures at the Micro- and Nanoelectronics Laboratory, Belarusian State University (5, Kurchatov Str., 220108, Minsk, Republic of Belarus). E-mail: parhomir@yandex.by

**Liudmila A. Vlasukova** – Ph. D. (Physics and Mathematics), Head of the Materials and Device Structures at the Micro- and Nanoelectronics Laboratory, Belarusian State University (5, Kurchatov Str., 220108, Minsk, Republic of Belarus). E-mail: vlasukova@bsu.by

**Natalia S. Kovalchuk** – Ph. D. (Engineering), Deputy Chief Engineer, Joint Stock Company “Integral” (121 A, Kazinets Str., 220108, Minsk, Republic of Belarus). E-mail: 7033696@mail.ru

**Fadei F. Komarov** – Corresponding Member, Dr. Sc. (Physics and Mathematics), Professor, Head of the Elionics Laboratory, A. N. Sevchenko Institute of Applied Physical Problems of the Belarusian State University (7, Kurchatov Str., 220108, Minsk, Republic of Belarus). E-mail: komarovf@bsu.by

**Oleg V. Milchanin** – Senior Researcher of the Elionics Laboratory, A. N. Sevchenko Institute of Applied Physical Problems of the Belarusian State University (7, Kurchatov Str., 220108, Minsk, Republic of Belarus). E-mail: milchanin@tut.by

**Maxim A. Makhavikou** – Junior Researcher of the Elionics Laboratory, A. N. Sevchenko Institute of Applied Physical Problems of the Belarusian State University (7, Kurchatov Str., 220108, Minsk, Republic of Belarus). E-mail: m.mohovikov@gmail.com

**Alexander V. Mudryi** – Ph. D. (Physics and Mathematics), Chief Researcher, Scientific and Practical Materials Research Center of the National Academy of Sciences of Belarus (19, Brovka Str., 220072, Minsk, Republic of Belarus). E-mail: mudryi@ifttp.bas-net.by.

**Vadim D. Zhivulko** – Junior Researcher, Scientific and Practical Materials Research Center of the National Academy of Sciences of Belarus (19, Brovka Str., 220072, Minsk, Republic of Belarus). E-mail: vad.zhiv@gmail.com.

**Hong-Liang Lu** – Ph. D. (Physics), Associate Professor, Department of Microelectronics at the Fudan University (220, Handan Rd., 200433, Shanghai, China). E-mail: honglianglu@fudan.edu.cn

### Информация об авторах

**Романов Иван Александрович** – аспирант факультета радиофизики и компьютерных технологий Белорусского государственного университета, младший научный сотрудник НИЛ «Материалов и приборных структур микро- и нанoeлектроники», Белорусский государственный университет (ул. Курчатова, 1, 220108, г. Минск, Республика Беларусь). E-mail: romivan@bsu.by

**Пархоменко Ирина Николаевна** – кандидат физико-математических наук, старший научный сотрудник НИЛ «Материалов и приборных структур микро- и нанoeлектроники», Белорусский государственный университет (ул. Курчатова, 5, 220108, г. Минск, Республика Беларусь). E-mail: parhomir@yandex.by

**Власукова Людмила Александровна** – кандидат физико-математических наук, заведующий НИЛ «Материалов и приборных структур микро- и нанoeлектроники», Белорусский государственный университет (ул. Курчатова, 5, 220108, г. Минск, Республика Беларусь). E-mail: vlasukova@bsu.by

**Ковальчук Наталья Станиславовна** – кандидат технических наук, заместитель главного инженера ОАО «Интеграл» (ул. Казинца, 121 А, 220108, г. Минск, Республика Беларусь). E-mail: 7033696@mail.ru

**Комаров Фадей Фадеевич** – член-корреспондент, доктор физико-математических наук, заведующий лабораторией элионики, Институт прикладных физических проблем им. А. Н. Севченко Белорусского государственного университета (ул. Курчатова, 7, 220108, г. Минск, Республика Беларусь). E-mail: komarovf@bsu.by

**Мильчанин Олег Владимирович** – старший научный сотрудник лаборатории элионики, Институт прикладных физических проблем им. А. Н. Севченко Белорусского государственного университета (ул. Курчатова, 7, 220108, г. Минск, Республика Беларусь). E-mail: milchanin@tut.by

**Моховиков Максим Александрович** – младший научный сотрудник лаборатории элионики, Институт прикладных физических проблем им. А. Н. Севченко Белорусского государственного университета (ул. Курчатова, 7, 220108, г. Минск, Республика Беларусь). E-mail: m.mohovikov@gmail.com

**Мудрый Александр Викторович** – кандидат физико-математических наук, главный научный сотрудник, Научно-практический центр Национальной академии наук Беларуси по материаловедению (ул. П. Бровки, 19, 220072, г. Минск, Республика Беларусь). E-mail: mudryi@ifttp.bas-net.by

**Живулько Вадим Дмитриевич** – младший научный сотрудник, Научно-практический центр Национальной академии наук Беларуси по материаловедению (ул. П. Бровки, 19, 220072, г. Минск, Республика Беларусь). E-mail: vad.zhiv@gmail.com

**Хонг-Лянгу Лу** – доктор философии (физика), доцент, Школа микроэлектроники Фуданского университета (220, Handan Rd., 200433, Shanghai, China). E-mail: honglianglu@fudan.edu.cn